ASEG-PESA 2013
'THE EUREKA MOMENT'
11-14 AUGUST 2013 · MELBOURNE, AUSTRALIA

Seismic and geoelectric study of the basaltic sequence in the south of Al-Madinah

Abdulrahman G. Alanezi
KACST
aenazi@kacst.edu.sa

Ayman N. Qadrouh
KACST
aqadrouh@kacst.edu.sa

SUMMARY

This study was carried out in Harat Rahat (south of Almadinah Almonwarah) using seismic reflection and resistivity methods. The main objectives of this study are to determine the extent of the basaltic layer and to define the subsurface faults and fractures that could affect and control the groundwater movement in the study area. A 2D seismic profile was acquired and the result shows that the subsurface in the study area has a major fault. We obtained a well match when the seismic result was compared with drilled wells. As a complementary tool, the resistivity method was applied in order to detect the groundwater level. The results of the resistivity method showed that six distinct layers have been identified. The interpretation of these six layers show that the first three layers, the fourth layer, the fifth layer and the bottom of the section indicated various subsurface structures and lithologies; various basaltic layers, fractured basalt, weathered basement and fresh basaltic layers, respectively. It is obvious that the eventual success of geophysical surveys depends on the combination with other subsurface data sources in order to produce accurate maps.

Key words: Seismic method, Vertical Electrical Sounding (VES), and Water table.

INTRODUCTION

The seismic reflection method has performed effectively to delineate the subsurface structures of the earth. Many authors such as Greenhalgh et al. (1986) and Knapp and Muftuoglu (1988) have detected coal using this method. Other researchers have utilized the seismic reflection method for a variety of applications. For instance, Philip et al. (2004) applied it to image a thin, diamondiferous kimberlite dyke. Clement et al. (2010) used it to delineate growth folding and shallow faults beneath the southern Puget lowland in Washington state. Cocker et al. (1997) used it to assist in mine planning and future horizontal drilling for coal-seam methane extraction.

Electrical resistivity methods have been successfully applied in ground investigations for several purposes. Their application in geotechnical and engineering site investigations were achieved by many geophysicists (Giao et al. (2003), Akintorinwa & Adesoji (2009), Ayolabi et al. (2010) and Folorunso et al. (2012)). Soil and groundwater were mapped by other investigators such as Cahyna et al. (1990) and Ayolabi et al. (2009). Khali (2009) utilized electrical resistivity methods to locate subsurface structures.

Mapping the extent of the basaltic layer and the subsurface structures were the main objectives of this study, which was

carried out by using seismic reflection, drilled wells and resistivity methods. The seismic results shows that the subsurface in the study area has a major fault as well as the efficiency of the seismic method to identify the water table level. The results of resistivity methods show that six distinct layers have been identified. Therefore, the results of seismic reflection and resistivity surveys are quite similar to the drilled wells.

FIELD PROCEDURES AND DATA PROCESSING

Seismic Reflection method

A 2D seismic profile was acquired using equipment and selected parameters based on the nature geological phenomena and area accessibility. Uncorrelated seismic data was recorded with 112 channels, where the geophone group interval and the shotpoint interval were 5m, and the offset between geophone and shotpoint was 10m, as shown in fig. 1. In addition, the selected field parameters in this study are shown in table1.

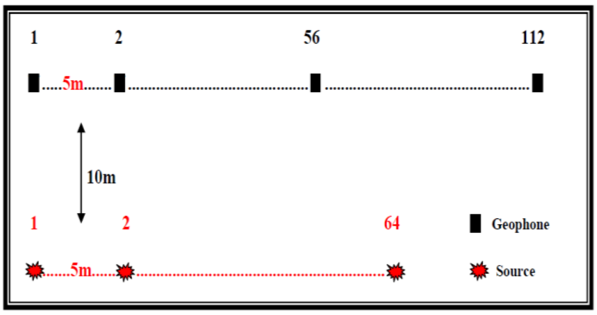

Fig.1. Shows the geometry of this study.

The primary objectives of seismic data processing are to produce high resolution images of the subsurface, achieved by enhancing signal to noise ratio and migrating the reflected waves to their correct position. The conventional processing sequence of seismic reflection data include, but are not limited to: filtering, statics application, deconvolution, CMP sorting, velocity analysis, NMO correction, stacking and migration. Flowchart 1 and fig. 2. show the stacked seismic section in time scale and the appropriate processing sequencing, in order to obtain better signal enhanced results respectively.

Table 1. The selected field parameters in this study

SPREAD	
Number of Traces	112 traces
Receiver interval	5 m
Source interval	5 m
Near offset	10 m
Max.offset	555 m
CDP fold	111 fold
SOURCE	
Type	Vibrosies
Model	Mini IVI
No. of Vibrator	One
Sweep type	Linear upsweep
Band width	20-300 Hz
Number of Sweep	1
RECEIVER	
Type	Geophone Flat base
Model	GS – 20 DH
Response	365 ohm , 40 Hz , 0.70 Damping
INSTRUMENTS	
Type	Geometrics , Strata Visor NZ
Sampling interval	0.5 ms
Gain constant	36 dB
Sweep length	5 s
Record length	2.5 s
Filter	out

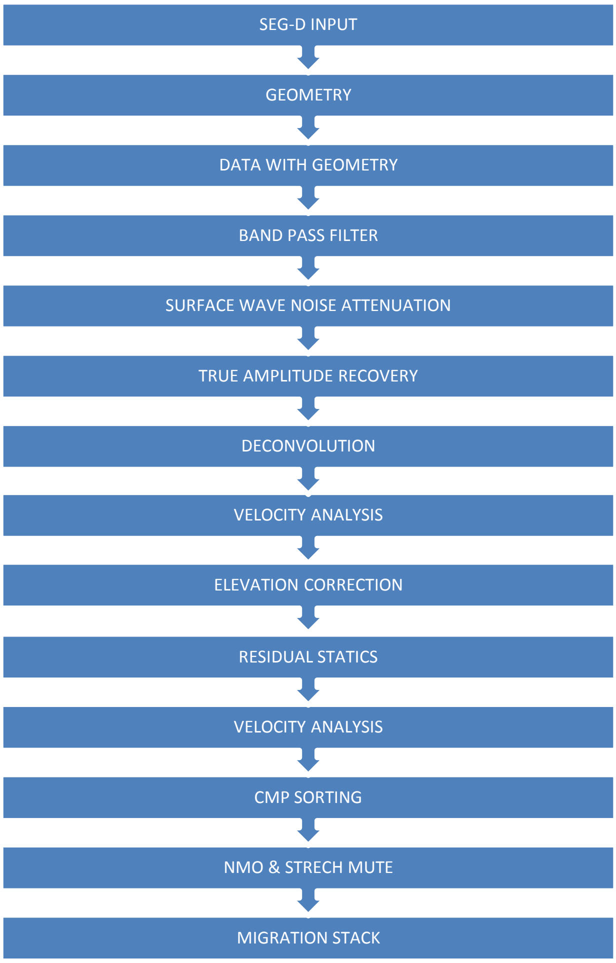

Flowchart.1. The processing steps in this research.

.

Electrical resistivity methods

The conventional equipment for resistivity surveys, such as an ammeter, voltmeter, power source, electrodes, and connecting wire were used in this research. In addition, we performed five vertical electrical soundings (VES) alone the seismic line in order to study the variation of resistivity with depth. Fig. 3. illustrates that this sounding was taken with the Schlumberger array, having a maximum separation of 1000m between the current electrodes, and the separation of the half current electrodes being gradually increased from 3 to 1000m. The maximum separation between potential currents was 120m, with increments started from 0.6

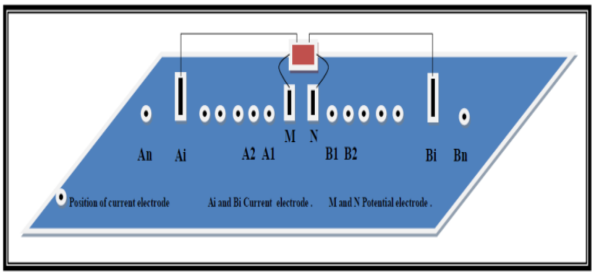

Fig 3. Sketch of the field setup for VES in Schlumberger array

The major steps in processing resistivity data consist of the following. First, producing a sounding curve which displayed the apparent resisitivities against the electrodes spacing, as illustrated in fig. 5. Next, the forward model in bars was created to show the curve of theoretical sounding corresponding to the model of the current earth as shown in figure 5. After that, building an inverse model which represented the curve of theoretical sounding corresponding to the model of the initial earth -and every subsequent trial model as convergence proceeded. Finally, the equivalence analysis was applied to indicate the earth models range that corresponded to the acquired data for the final inverted model, as revealed in fig. 6. Note that the processing of the first VES is represented here. This is due to the fact that the processing sequence for the others were quite similar to steps for the first VES.

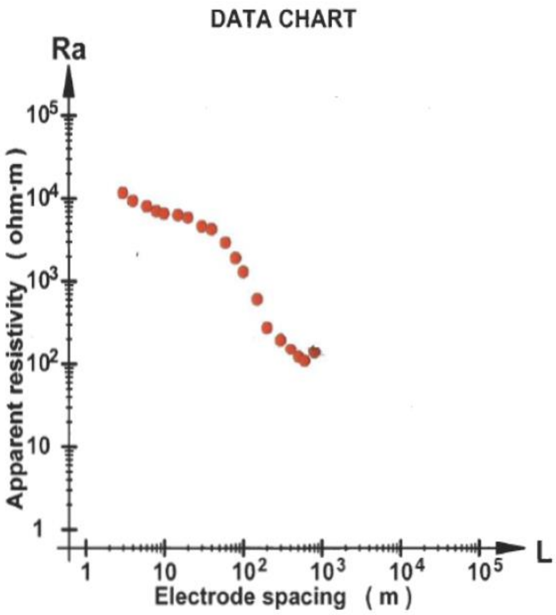

Fig. 4. Sounding curve

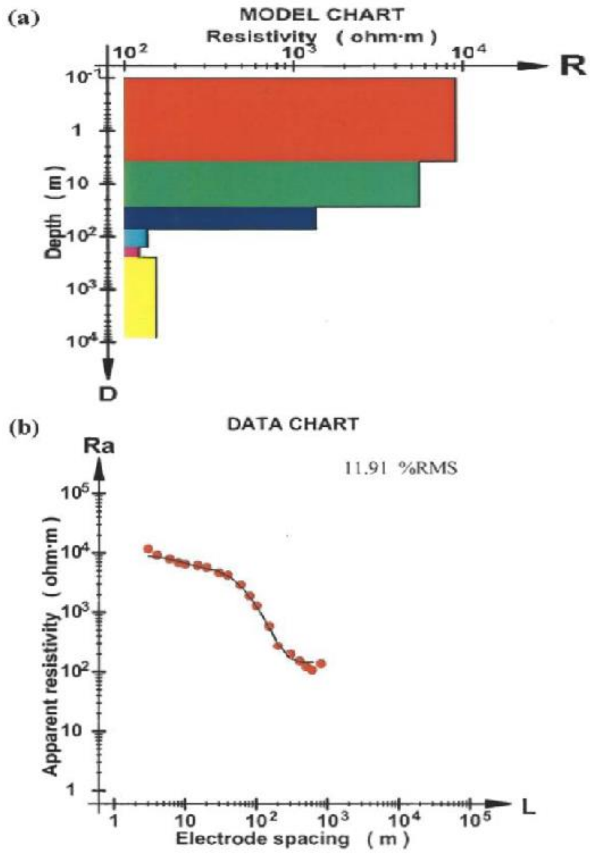

Fig. 5. The forward model in comparison with data

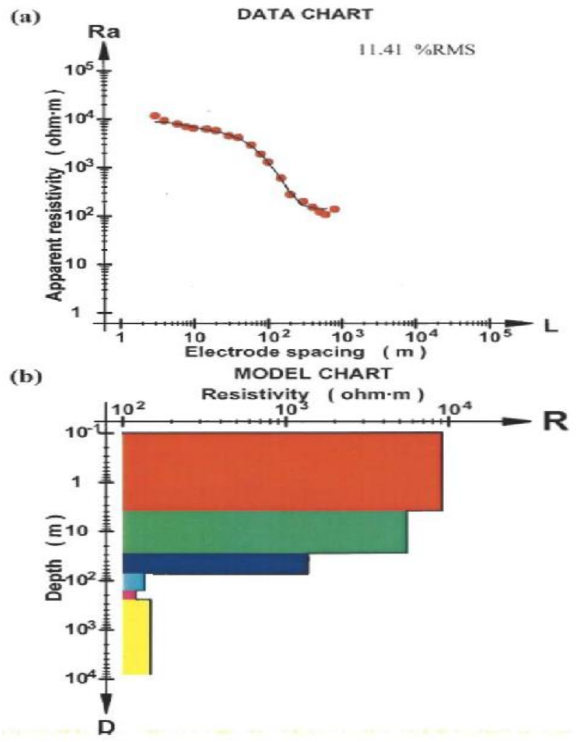

Fig. 6. The inverted model in comparison with data

Interpretation of the results

Seismic Data Interpretation

The seismic section was interpreted in order to identify the water table layer across the survey area. The interpretation began by transforming the stacked section from time (ms) to depth (m), where the accuracy of such depth conversion depends on how accurate the processing of seismic data is; that is to say, accurate depth conversion depends on the accuracy of velocities and times recorded. We applied the interval velocity approach to convert the data from time to depth scale. The stacked section shows that the subsurface in the study area has a major fault. In addition, the results of the seismic section show that there are two seismic reflectors, where the second reflector is associated with a water table at a depth range of 125m to 230m. This reflector is considered the surface of the third seismic layer that represents groundwater saturated fractured basalts. The abrupt and remarkable increase in the depth of the second layer is due to faulting in the area between 40 and 260 m distant from the shot point. In order to reach a more accurate depth interpretation than that presented only by seismic section, we tied five drilled wells(W-1,W-2,W-7,W-11, and W-12) to the seismic data as shown in fig. 7. Table 2 demonstrates the detail information about the five drilled wells integrated with stacked section to mark the water table layer related horizon. W-1 and W-2 are dry wells because they are at a shallow depth of 135m, while the water table layer is located at a depth of 230m. The water layer is found in W-7, W-11 and W-12 at depth 125m, 150m, and 150m respectively.

Table 2: The information of the five drilled wells

Wells information	W-7	W-1	W-2	W-11	W-12
Distance from 1st Geophone (m)	117	342	530	800	1155
Water table depth (m)	125	135	135	150	150

Resistivity Data Interpretation

The interpretations of the five VES stations show that the area under study has six layers. The first layer is a thin layer of very dry weathered basalt, with an average value of ρ =8430 Ohm.m, and at a depth ranging from 1 to 7.5 m. The value of apparent resistivity in the second layer is about ρ>4000 Ohm.m and at depth ranging from 7.5 to 20 m, which might be comprised of fresh basalt. The third layer has an apparent resistivity value between 1000 to 1200Ohm.m and at a depth range of 20 to 60m. This layer was interpreted as fresh water saturated fractured basalt, intercalated with some gravelly sand. The analysis of the fourth layer showed that the values of apparent resistivity are between 150 and 200Ohm.m and with a depth range of 60 to 155m. This layer was characterized as fractured basalt with clay saturated with salt-water. The values of the apparent resistivity in the fifth layer were between 100 and 120 Ohm.m and the depth range was 126 to 184 m. This layer was interpreted as a weathered basement. The sixth layer had an apparent resistivity ρ >300 Ohm.m, and which was interpreted as compact basement.

Conclusion

The geophysical methods used allowed us to identify the subsurface structures, to obtain lithological information, and to characterize the conditions of the underground flow in the studied area. The interpretation of seismic data was agreed with the available drilled wells to locate the water table depths which varied generally between 120m to 150m, as well as the effectiveness of the seismic method to detect the surface fault. In addition, the resistivity method located the various lithologies in the subsurface, such as different basaltic layers, fractured basalt, weathered basement and fresh basaltic layers respectively. It is clear that the ultimate success of geophysical surveys depends on the inclusion other subsurface data sources in order to produce precise maps.

ACKNOWLEDGMENTS

The authors wish to thank KACST for their wealth of knowledge and valuable data for this research.

REFERENCES

Akintorinwa, O. J., & Adesoji, J. I. (2009). Application of geophysical and geotechnical investigations in engineering site evaluation. *Pacific Journal of Science and Technology, USA, 10*(2), 680-692.

Ayolabi, E. A., Atakpo, E. A., Adeoti, L., Otobor, E. C., & Arerin, T. (2009b). Groundwater quality assessment using predrilling electrical measurements. *Journal of Environmental Hydrology, 17*, 1-12.

Ayolabi, E. A., Folorunso, A. F., & Oloruntola, M. O. (2010c). Constraining causes of structural failure using electrical resistivity tomography (ERT): A case study of lagos, southwestern, Nigeria. *Mineral Wealth, Greece, 156*, 7-18.

Cahyna, F., Mazac, O., & Vendhova, D. (1990). Determination of the extent of cyanide contamination by surface geo-electrical methods. *SEG-Geotechnical and environmental Geophysics, Tulsa., 2*, 97-99.

Clement, C. R, Pratt, T. L, Holmes, M. L & Sherrod, B. L 2010, High-Resolution Seismic Reflection Imaging of Growth Folding and Shallow Faults beneath the Southern Puget Lowland, Washington State, Bulletin of the Seismological Society of America, vol. 100, pp. 1710-1723.

Cocker, J, Urosevic, M & Evans, B 1997, A high resolution seismic survey to assist in mine planning: Proceeding of fourth decennial international conference on mineral exploration, edited by A. G. Gubins, pp. 473 - 476.

Folorunso, A. F., Ayolabi E. A., Ariyo, S. O., & Oyebanjo, I. O. (2012). Fault presence under a failing building complex mapped by electrical resistivity tomography. *Mineral Wealth*, Greece .

Giao, P. H., Chung, S. G., Kim, D. Y., & Tanaka, H. (2003). Electrical imaging and laboratory resistivity testing for geotechnical investigation of Pusan clay deposits. *Journal of Applied Geophysics, 52*, 157-175.

Greenhalgh, S, Suprajitno, M & King, D 1986, Shallow seismic reflection investigations of coal in the Sydney Basin, Geophysics, vol.v51, pp. 1426-1437.

Khalil, M. H. (2009). Hydrogeophysical assessment of wadi el-sheikh aquifer, saint katherine, south Sinai, Egypt. *Journal of Environmental and Engineering Geophysics, JEEG, 14*(2), 77-86.

Knapp, R & Ertan Muftuoglu, A (1987), Detection of coals 30 cm thick at depths of 50 and 60 m by seismic reflection profiling. SEG Technical Program Expanded Abstracts 1987: pp. 227-228.

Philip T.C. H, Ron M.C and Kumar R 2004, High-resolution seismic reflection imaging of a thin, diamondiferous kimberlite dyke, Geophysics, vol. 69, pp. 1143-1154.

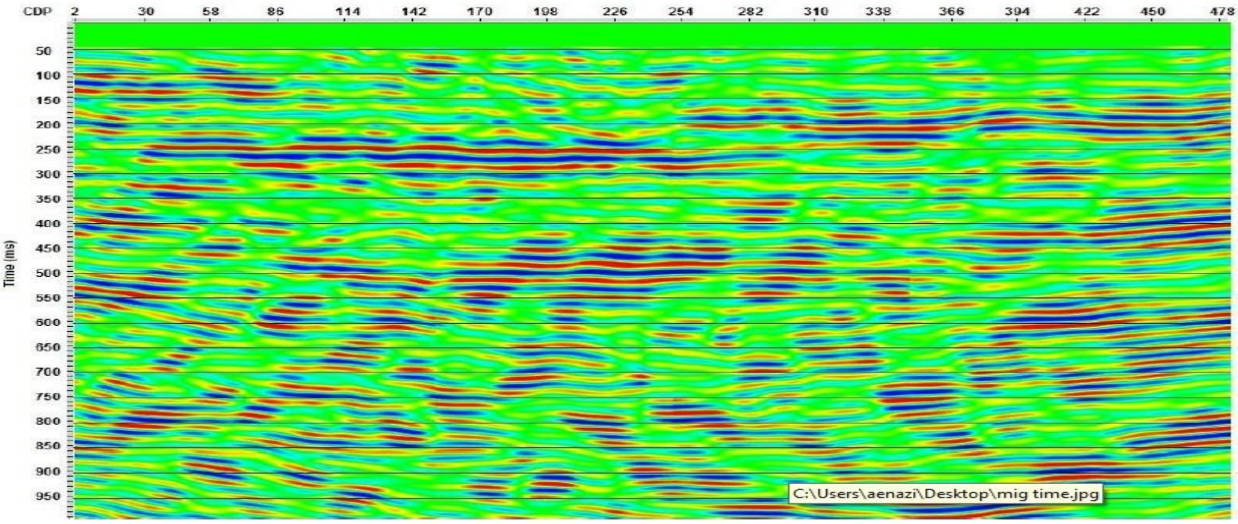

Fig. 2. The stacked seismic section in time scale.

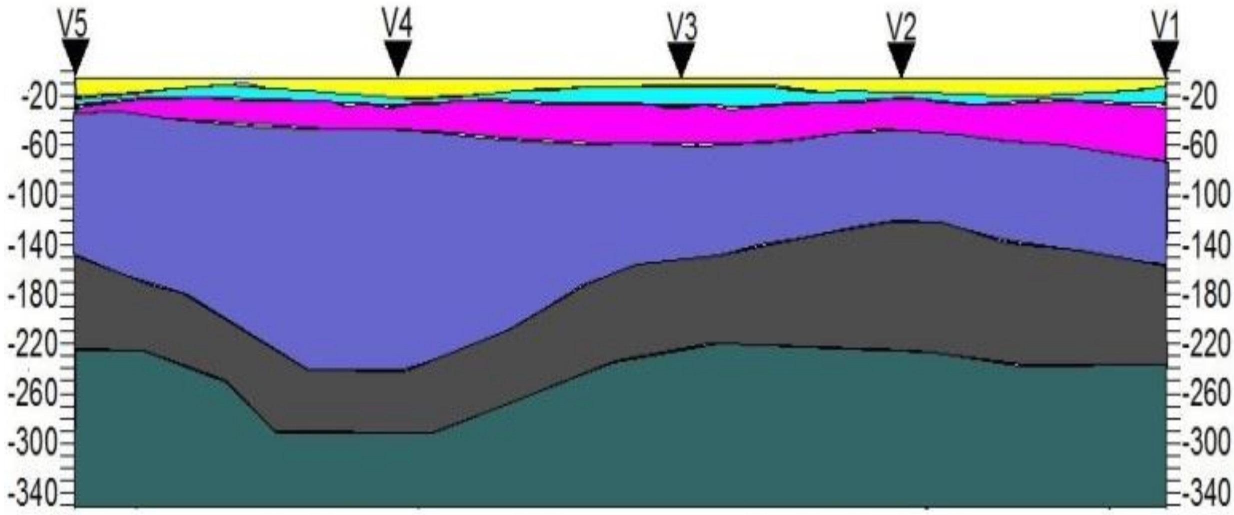

Fig. 8. This composite diagram show data from seismic and VES

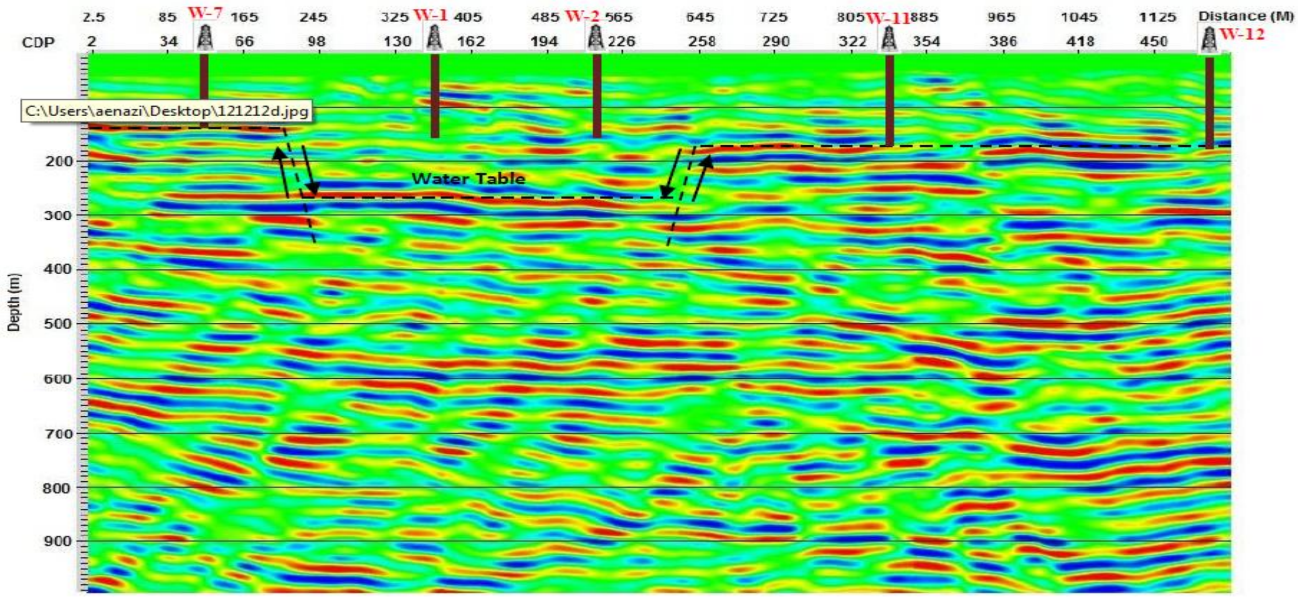

Fig. 7. Interpreted Stack (Depth) .